Geoscience Letters

RESEARCH LETTER

Open Access

Using ensemble quantitative precipitation forecast for rainfall-induced shallow landslide predictions

Jui-Yi Ho[1*], Che-Hsin Liu[1], Wei-Bo Chen[1], Chih-Hsin Chang[1] and Kwan Tun Lee[2,3]

Abstract

Heavy rainfall brought by typhoons has been recognised as a major trigger of landslides in Taiwan. On average, 3.75 typhoons strike the island every year, and cause large amounts of shallow landslides and debris flow in mountainous region. Because landslide occurrence strongly corresponds to the storm dynamics, a reliable typhoon forecast is therefore essential to landslide hazard management in Taiwan. Given early warnings with sufficient lead time, rainfall-induced shallow landslide forecasting can help people prepare disaster prevention measures. To account for inherent weather uncertainties, this study adopted an ensemble forecasting model for executing precipitation forecasts, instead of using a single-model output. A shallow landslide prediction model based on the infinite slope model and TOPMODEL was developed. Considering the detailed topographic characteristics of a catchment, the proposed model can estimate the change in saturated water table during rainstorms and then link with the slope-instability analysis to clarify whether shallow landslides can occur in the catchment.

Two areas vulnerable to landslide in Taiwan were collected to test the applicability of the model for landslide prediction. Hydrological data and landslide records derived from 15 typhoons events were used to verify the applicability of the model. Three indices, namely the probability of detection (POD), false alarm ratio (FAR), and threat score (TS), were used to assess the performance of the model. The results indicated that for landslide prediction through the proposed model, the POD was higher than 0.73, FAR was lower than 0.33, and TS was higher than 0.53. The proposed model has potential for application in landslide early warning systems to reduce loss of life and property.

Keywords: Saturated water table, Shallow landslide, Early warning

Introduction

Taiwan is located on the primary path of typhoons that develop in the Northwest Pacific Basin. According to Taiwan's Central Weather Bureau (CWB), Taiwan has experienced, on average, three to four typhoons annually in the past century. The steep topography and weak geological structures in mountainous areas in Taiwan have frequently been subjected to landslides and mudflows during typhoons accompanied by abundant rainfall. For example, Typhoon Soudelor that occurred in August 2015 induced seven landslide and mudflow incidents in the mountainous areas of Xindian and Wulai and resulted in road blockage and isolation of the affected area. Therefore, using precipitation forecasts in mountainous areas to establish accurate landslide warning systems with timely alarms is imperative to mitigate loss of life and property.

To effectively mitigate losses engendered by typhoon- and rainstorm-induced landslides, adequate warning systems and contingency measures are required to supplement the necessary engineering methods so that updated information about typhoons and rainstorms can be obtained before a disaster occurs (Guzzetti et al. 2020). Therefore, precise quantitative precipitation forecasts and landslide simulation

*Correspondence: juiyiho@ncdr.nat.gov.tw

[1] National Science and Technology Center for Disaster Reduction, New Taipei City, Taiwan
Full list of author information is available at the end of the article

capability are paramount to landslide warning systems and disaster prevention. Recently proposed forecasting technologies for typhoon-induced rainfall can be broadly divided into two types according to the underlying theoretical foundation: physically based and statistically based forecasting models. Physically based forecasting models are based on aerodynamic theories, and they produce typhoon precipitation forecasts through numerical computation. Therefore, such models can account for a more comprehensive physical framework to simulate and forecast typhoon-induced precipitation. The Taiwanese research community has employed the Fifth-Generation Mesoscale Meteorological Model (MM5) codeveloped by Pennsylvania State University and the National Center for Atmospheric Research (NCAR) and a new-generation mesoscale weather research and forecasting (WRF) model developed by the NCAR to conduct ensemble simulations of approaching typhoons by using physical parameters. The results have demonstrated that selecting suitable physical parameters enables effectively simulating typhoon paths and rainfall distributions. Because of the limitations of numerical weather forecasting models and the variability of the atmosphere, single-model forecasts involve uncertainties to a certain extent and cannot attain completely accurate prediction of actual weather conditions. Therefore, systematic analyses and research involving optimal model combinations are required to develop ensemble forecasting techniques and mitigate the uncertainties associated with atmospheric forecasts. Major forecasting centres worldwide have actively developed both global and regional ensemble forecasting systems. For example, the European Centre for Medium-Range Weather Forecasts generates 15-day global forecasting products daily with 51 ensemble units, and the objective uncertainties of typhoon paths provided by these products play a crucial role in the CWB's practical forecasting operations. In the United States, the National Centers for Environmental Prediction provide 16-day forecasts daily with 88 ensemble units. In Asia, the Japan Meteorological Agency employs a global medium-range ensemble prediction model with 51 units and 40 vertical levels, whereas the Korea Meteorological Administration uses a global ensemble forecasting model with 32 units and 40 vertical levels (Li and Hong 2011).

For landslide warning, conventional methods predominately entail using historical rainfall data and documenting landslide incidents to statistically calculate the threshold rainfall amount for landslide warning tasks. For example, Caine (1980) and Hong et al. (2006) have collected high-intensity and long-duration rainfall data in slopes worldwide and determined the critical relationship between the lower boundary of these data points and landslide occurrence through statistical regressions. Cannon and Ellen (1985) and Wieczorek (1987) have employed the same method to investigate the relationship between landslides and rainfall by using data for multiple landslides in the San Francisco Bay Region and a landslide incident in La Honda, California, respectively. Subsequently, Keefer et al. (1987) adopted the data collected by the two aforementioned studies as well as those collected by Caine (1980) to construct the critical rainfall conditions associated with landslides by using the relationship between rainfall intensity and duration. Lee et al. (2008) used multivariate statistical methods to solve a regional landslide susceptibility model; they trained the proposed model using data for Typhoon Toraji in 2001 and then validated the model using data for Typhoon Mindulle in 2004. The analysis results revealed that the maximum rainfall intensity was the triggering factor in the proposed model and yielded favourable landslide predictions in Central Taiwan. Silalahi et al. (2019) used the GIS mapping and analysis a Frequency Ratio Model to assess the contribution of conditioning factors to landslides, and to produce a landslide susceptibility map in Bogor, West Java, Indonesia. However, statistically based landslide warning systems have limitations because regional differences in sediment, catchment area slope grade, geological conditions, landform types, and climatic conditions may lead to varying rainfall conditions triggering landslides.

Physically based models for evaluating slope stability in catchment areas typically apply the infinite slope model (Skempton and DeLory 1957). This model applies the ratio of the sediment resistance force τ_r to the sediment driving force τ_d to calculate the factor of safety ($FS = \tau_r / \tau_d$), which is then used to evaluate whether a landslide will occur. For example, Iverson (2000) used simplified forms of Richards equation to calculate saturated and unsaturated rain infiltration without considering the effect of excess rainfall. In addition, Iverson used the infinite slope stability analysis to simulate slope destructions caused by increased saturated water levels. Casadei et al. (2003) combined the infinite slope model with a hydrological model to simulate the time and location of shallow landslides in catchment areas in San Mateo County, California, by using daily precipitation data from 1950 to 1998. The development of geographic information systems in recent years has enabled the incorporation of high-resolution spatial information—such as physiographic, hydrological, and land-use data—into topographic hydrological models based on the infinite slope model and thus facilitated landslide hazard simulations (Lee and Ho 2009; Ho and Lee 2017).

The current study employed a quantitative ensemble forecasting model to compensate for the limitations of single-model forecasts. The proposed model comprises multiple ensemble units and is expected to account for and quantify the uncertainties associated with single-model forecasts to provide precipitation forecasts. In addition, the

proposed model incorporates a physically based hydrological model and a digital elevation model (DEM) to account for catchment situations, thereby establishing a landslide warning system for catchment areas. The landslide warning system reflects the precipitation, topography, and water flow in catchment areas and analyses changes in saturated water levels and slope *FS* to calculate the potential location and time of landslides. The proposed model can expedite landslide analysis before future slope disasters occur to ensure that the time and range of potential disasters can be understood. Moreover, the proposed model can serve as a reference for relevant departments in implementing disaster response strategies to ensure the safety of life and properties.

Methodology

This study adopted the Shallow landslide prediction based on Infinite slope Model and TOPMODEL (SIMTOP) developed by Ho and Lee (2017) to simulate shallow landslides. This enabled constructing a topographic hydrological model and a slope stability model to simulate changes in the saturated water level on the surface soil of a catchment area and the FS of slope during rainfall periods. The simulated data can be used to predict the time and location of a landslide in the catchment area. To increase the disaster lead time, this study combined SIMTOP with the TAiwan cooperative Precipitation Ensemble forecast eXperiment (TAPEX) to construct a comprehensive real-time shallow landslide warning system for catchment areas. In addition, this study employed three evaluation indices to analyse the performance of the proposed model. The related research methods are described as follows.

Ensemble precipitation forecasts

Because weather forecasts have regional characteristics and uncertainties and because overseas research outcomes cannot be directly adapted to domestic situations, extensive analysis and research procedures are required to summarise the optimal model and settings most suitable for the complex terrain features in Taiwan. As presented in Fig. 1, the objective of the TAPEX, which has been conducted by the Taiwan Typhoon and Flood Research Institute (TTFRI) since 2010, is to research and develop quantitative ensemble forecasting technologies and provide a reference for disaster prevention agencies in coordinating response tasks, thereby enhancing effectiveness of disaster rescue operations. This experiment combines the research capacity of academia National Taiwan University (NTU), National Central University (NCU), National Taiwan Normal University (NTNU), and Chinese Culture University (CCU)) and a meteorological agency (CWB), as well as the computing resource of the National Center for High-performance Computing (NCHC) and practical experience of the National Science and Technology Center for Disaster Reduction (NCDR). During typhoon seasons in Taiwan, the TAPEX generates real-time weather forecasts and analyses typhoon paths and rainfall distributions through ensemble statistical methods and probabilistic forecasting concepts to determine the probability of disaster-triggering rainfall (Hsiao et al. 2013). The TAPEX expanded the roster of ensemble units to 27, comprising 21 WRF models, 2 MM5 models, 2 Cloud Resolving Storm Simulator models, and 2 hurricane weather research and forecasting models. The present study adopted the TAPEX results and combined real-time data observed by various rainfall stations to derive

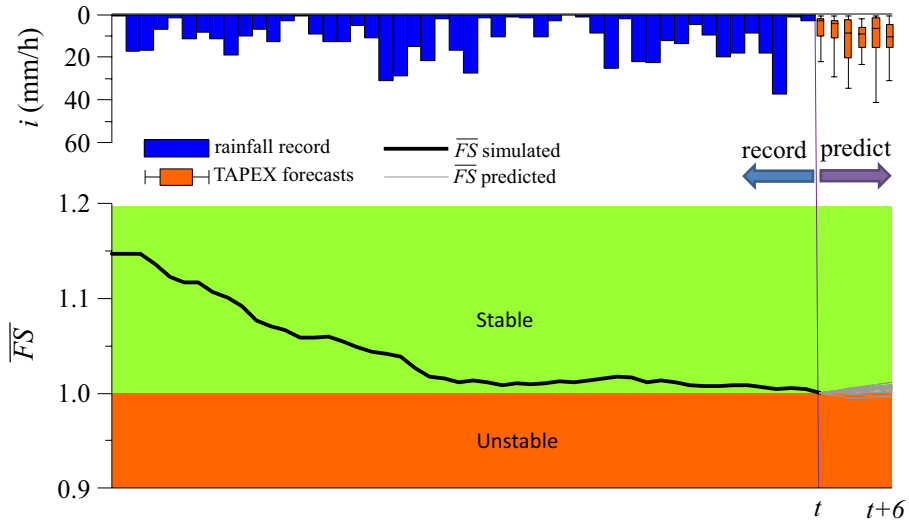

Fig. 1 Display of TAPEX-SIMTOP model's platform

hourly rolling updates that serve as the input to the real-time shallow landslide warning system for catchment areas.

SIMTOP model

SIMTOP model (Ho and Lee 2017) applies the infinite slope stability theory of Mohr–Coulomb failure law to estimate the susceptibility of a landslide. This analysis involves using the factor of safety (FS) as expressed by the ratio of resistance force (τ_r) to driving force (τ_d) on a failure plane parallel to the ground surface. The dimensionless factor of safety can be expressed as follows:

$$FS = \frac{\tau_r}{\tau_d} = \frac{\tan\phi}{\tan\beta} + \frac{c}{\rho_s g D \sin\beta\cos\beta} + \frac{-\rho_w D_w(t)\tan\phi}{\rho_s D \tan\beta}, \tag{1}$$

where ϕ is the friction angle; β is the inclination of the hillslope; c is the effective cohesion (N/m^2); ρ_s is the soil bulk density (kg/m^3); g is the gravity acceleration (=9.81 m/s^2); D is the thickness of soil (m); ρ_w is the water density (kg/m^3); $D_w(t)$ is the saturated water level at the time t (m). When FS = 1 (i.e. $\tau_r = \tau_d$), the slope soil is in a critical state. When $FS < 1$ (i.e. $\tau_d > \tau_r$), the slope soil is in an instable state, implying that it is prone to sliding or collapsing. Conversely, when $FS > 1$ (i.e. $\tau_r > \tau_d$), the slope soil is in a stable state. Equation (1) has been extensively used for evaluating slope stability (Montgomery and Dietrich 1994; Wu and Sidle 1995; Casadei et al. 2003; Apip et al. 2010; Zizioli et al. 2013).

Equation (1) indicates that the FS changes with the saturated water level, and this equation can be used to analyse the slope stability of catchment areas by simulating $h_w(t)$ in a topographic hydrological model. This study selected the topographic and semi-distributed TOPMODEL (TOPography-based hydrological model) developed by Beven and Kirkby (1979) for rainfall–runoff simulations in a catchment area. When the accumulated rainfall exceeds the infiltration capacity, the saturated water level gradually increases. Therefore, the distance between the ground surface and a saturated aquifer can be estimated by considering the topographic and soil conditions of the catchment area. The topographic index model divides the runoff storage reservoir into a root zone, unsaturated zone, and saturated zone and defines the distance between the ground surface and saturated aquifer as the saturated water level z_j. Therefore, the saturated water level above the sliding surface (h_{w_j}) can be expressed as follows:

$$D_{w_j}(t) = D_j - z_j(t) = D_j - \bar{z}(t) - m\left[\lambda - \ln\left(\frac{a}{\tan\beta}\right)_j\right], \tag{2}$$

where $h_{w_j}(t)$ is the saturated water level on grid j at time t; D_j is the soil thickness on grid j; $\bar{z}(t)$ is the mean saturated water level at time t; m is the model coefficient obtained using water recession records; a and $\tan\beta$ are the area and surface slope of unit width flow on j, respectively; $\ln(a/\tan\beta)_j$ is the topographic index on j (Kirkby 1975); and λ is the mean topographic index of the catchment area. The mean saturated water depth at time $t+1$ can be expressed as follows:

$$\bar{z}(t+1) = \bar{z}(t) + Q_b(t)\cdot\Delta t - Q_v(t)\cdot\Delta t, \tag{3}$$

where $\bar{z}(t)$ is the mean saturated water depth at time t, $Q_b(t)$ is the outflow from the saturated zone in the catchment outlet at time t, and $Q_v(t)$ is the mean replenishment of the saturated zone at time t.

The infinite slope model executes grid computing and determines grid stability through the FS. However, in practice, neighbouring grids may mutually affect each other (e.g., unstable grids may be affected by adjacent stable grids and thus display a stable state). To mitigate the interaction between grids, this study applied the mean FS of the catchment area to determine the occurrence of shallow landslides, and Eq. (1) can be rewritten as follows (Ho and Lee 2017):

$$\overline{FS}(t) = \frac{1}{N}\sum_{j=1}^{N}\left(\frac{C_j}{\rho_s g D_j \sin\beta_j\cos\beta_j} + \frac{\tan\phi_j}{\tan\beta_j} - \frac{\left[D_j - \bar{z}(t) - m\left(\lambda - \ln\left(\frac{a}{\tan\beta}\right)_j\right)\right]\rho_w\tan\phi_j}{\rho_s D_j \sin\beta_j\cos\beta_j}\right), \tag{4}$$

where $\overline{FS}(t)$ is the mean FS of the catchment area at time t and N is the number of grids in the catchment area. When $\overline{FS}(t) < 1$, the overall soil driving force exceeds the resistance force at time t, indicating an unstable state of the slope soil in the catchment area, which might lead to shallow landslides. Conversely, when $\overline{FS}(t) > 1$, the overall soil driving force is lower than the resistance force at time t, indicating a stable state of the slope soil.

TAPEX–SIMTOP integration

This study adopted the 20 sets of rainfall forecasts generated by the TTFRI and NCDR combined real-time rainfall data observed by rainfall stations to derive rolling updates of rainfall forecasts with a 6-h lead time (as shown in Fig. 1). Moreover, this study derived the mean FS of all ensemble units for the upcoming 1–6 h in the catchment area through real-time SIMTOP computation. The mean FS can be expressed as follows:

$$\left\{\begin{array}{l} m_1\left[\overline{FS}_{T=t+1h}\right]\ m_2\left[\overline{FS}_{T=t+1h}\right]\ \ldots\ m_{20}\left[\overline{FS}_{T=t+1h}\right] \\ m_1\left[\overline{FS}_{T=t+2h}\right]\ m_2\left[\overline{FS}_{T=t+2h}\right]\ \ldots\ m_{20}\left[\overline{FS}_{T=t+2h}\right] \\ m_1\left[\overline{FS}_{T=t+3h}\right]\ m_2\left[\overline{FS}_{T=t+3h}\right]\ \ldots\ m_{20}\left[\overline{FS}_{T=t+3h}\right] \\ m_1\left[\overline{FS}_{T=t+4h}\right]\ m_2\left[\overline{FS}_{T=t+4h}\right]\ \ldots\ m_{20}\left[\overline{FS}_{T=t+4h}\right] \\ m_1\left[\overline{FS}_{T=t+5h}\right]\ m_2\left[\overline{FS}_{T=t+5h}\right]\ \ldots\ m_{20}\left[\overline{FS}_{T=t+5h}\right] \\ m_1\left[\overline{FS}_{T=t+6h}\right]\ m_2\left[\overline{FS}_{T=t+6h}\right]\ \ldots\ m_{20}\left[\overline{FS}_{T=t+6h}\right] \end{array}\right\}, \quad (5)$$

where m_i is the ith ensemble unit ($i = 1 \sim 20$). In addition, to determine whether the rainfall forecast by each ensemble unit would lead to shallow landslides, a unit step function was used as follows:

$$I_i = \begin{cases} 1 \text{ if } m_i\left[\overline{FS}_{T=t+1\sim6h}\right] < 1 \text{ Unstable} \\ 0 \text{ if } m_i\left[\overline{FS}_{T=t+1\sim6h}\right] \geq 1 \text{ Stable} \end{cases}. \quad (6)$$

If the mean FS derived for an ensemble unit for the upcoming 6 h is < 1 ($m_i\left[\overline{FS}_{T=t+1\sim6h}\right] < 1$), the unit step function can be set as 1 ($I_i = 1$). Consequently, the rainfall forecast by this ensemble unit for the upcoming 6 h would cause the slope driving force to exceed the resistance force; this would thus result in an unstable state of the soil and thereby predict a shallow landslide in the catchment area. Conversely, if the FS derived for an ensemble unit for the upcoming 6 h is ≥ 1 ($m_i\left[\overline{FS}_{T=t+1\sim6h}\right] \geq 1$), the unit step function can be set as 0 ($I_n = 0$). Consequently, the rainfall forecast by this member (m_i) for the upcoming 6 h would cause the driving force to be lower than the resistance; this would result in a stable state of the slope soil in the catchment area. In addition, this study incorporated probabilistic forecasting into the analysis and summarised the outcomes of all ensemble units to calculate the probability of shallow landslides as follows:

$$P_{T=t+1\sim6h} = \frac{1}{n}\left[I_{1,T=t+1\sim6h} + I_{2,T=t+1\sim6h} + \ldots + I_{n,T=t+1\sim6h}\right], \quad (7)$$

where $P_{t=1-6h}$ is the probability of shallow landslides (ranging between 0 and 1) for the upcoming 6 h. In the proposed system, a threshold of 0.5 is set for the probability of shallow landslides: when $P_{T=t+1\sim6h} \geq 0.5$, the system determines that shallow landslides will occur (i.e. the majority of the ensemble units determine a landslide hazard); conversely, when $P_{T=t+1\sim6h} < 0.5$, the system determines that the catchment area is in a stable state.

Evaluation indices

To evaluate the performance of each model in shallow landslide prediction, the forecast results obtained from the models were compared with actual observation data, and an error matrix was constructed to determine the accuracy of each model. The error matrix comprised four categories (Table 1): hits (successful landslide prediction), misses (failure to predict a landslide), false alarms (predicted landslide while no actual landslide occurred), and no events (no landslide prediction and no actual landslide). Therefore, the error matrix results were used to calculate three evaluation indices, namely the probability of detection (POD), false alarm ratio (FAR), and threat score (TS), to verify the applicability of SIMTOP. These indices can be derived as follows (Wilks 2005; Schaefer 1990):

$$\text{POD} = \frac{\text{hits}}{\text{hits} + \text{misses}}. \quad (8)$$

Table 1 Error matrix

	Landslide occurrence (Predicted)	Non-landslide occurrence (Predicted)
Landslide occurrence (Observed)	hits	misses
Non-landslide occurrence (Observed)	false alarms	no events

$$\mathrm{FAR} = \frac{\text{false alarms}}{\text{hits} + \text{false alarms}}, \tag{9}$$

$$\mathrm{TS} = \frac{\text{hits}}{\text{hits} + \text{false alarms} + \text{misses}}. \tag{10}$$

The POD, as presented in Eq. (8), ranges between 0 and 1 and represents the proportion of successful predictions of shallow landslide events. A POD value closer to 1 indicates higher model prediction performance. However, because the POD is derived by considering only hits while ignoring false alarms, a smaller sample size may generate an overstated POD value. Therefore, the FAR is typically included in performance assessments. The FAR, as presented in Eq. (9), represents the proportion of false alarms for an event under evaluation. An FAR value closer to 0 indicates higher model prediction performance. Finally, the TS, as presented in Eq. (10), ranges between 0 and 1 and is evaluated by considering both false alarms and misses; this index can be considered as representing the model prediction accuracy. The TS value closer to 1 indicates higher model prediction performance; the TS value is equal to 0 when the model exhibits no predictive capability.

Description of study areas

To demonstrate the capability of the proposed SIMTOP with TAPEX model, hydrological records and geomorphological factor from two landslide-prone areas in Taiwan were collected to conduct the slope-instability analysis and their prediction. The Chung-Chih (C1) and Dong-Yen (C2) villages are selected as the study areas for testing the applicability of the proposed model in this study.

Chung-Chih village catchment (C1)

The rainstorm engendered by Typhoon Soudelor (2015) caused considerable damage in Wu-Lai District of New Taipei City in northern Taiwan. Specifically, severe shallow landslides and mudflows occurred along the 9.8–10.2 km marks of Provincial Highway 9A in Chung-Chih village and disrupted the road transportation of the mountainous area, thus isolating Wu-Lai District and endangering local residents' safety and properties. Therefore, Chung-Chih Village of Wu-Lai District was selected as the study area. Chung-Chih Village (C1) is located in the Nan-Shi River watershed (Fig. 2). The Nanshi River watershed has an average elevation of approximately 870 m (maximum elevation = 2210 m) and an average slope of approximately 0.562. The entire region is covered by Tertiary metamorphic rocks, and the geological formations include the Tatungshan Formation (argillite mixed with argillaceous sandstones), Kangkou Formation (argillite mixed with sandstones with varying thickness), Lateritic Terrace Deposits Formation (laterite, gravel, sand, and clay), Fangjiao section of Aoti Formation, Hsitsun Formation, and Baling Formation. To determine the applicability and parameters of the proposed model, this study

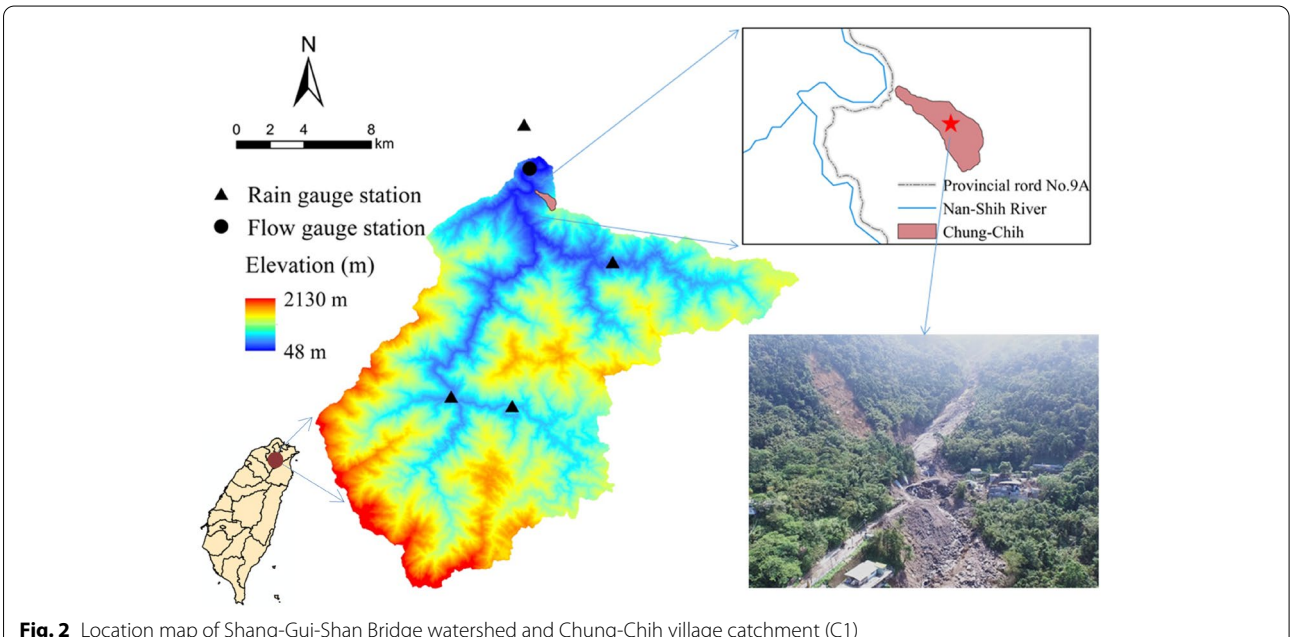

Fig. 2 Location map of Shang-Gui-Shan Bridge watershed and Chung-Chih village catchment (C1)

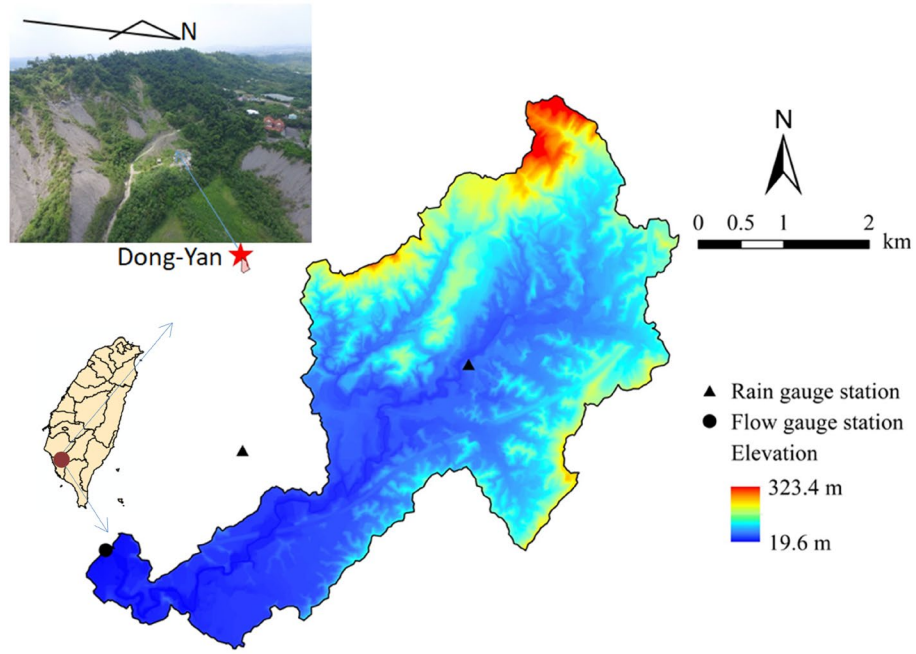

Fig. 3 Location map of Yeng-Feng Bridge watershed and Dong-Yen village catchment (C2)

selected the Shang-Gui-Shan Bridge watershed area in the downstream of the Nan-Shi River as the sample catchment area. Rainfall and flow discharge data were used to verify the hydrological parameters of SIMTOP model. The study area is 0.59 km^2 and average slope is 0.724. This area was subjected to multiple typhoons and rainstorms between 2010 and 2016, including three severe shallow landslides caused by Typhoon Soudelor (2015), Typhoon Dujuan (2016), and Typhoon Megi (2016).

Dong-Yen village catchment (C2)

Figure 3 illustrates the Dong-Yen village catchment, which is located in southern Taiwan and was selected as one of model test regions. During 27–28 September 2016, Typhoon Megi caused a shallow landslide in the Dong-Yen village resulting three people deaths. The shallow landslide occurred at about 7 p.m. as 521.5 mm fell in single day and maximum hourly rainfall intensity up to 74.5 mm/hr. The landslide scale is about 145 m in length, 30 m in width, 2 m in depth, and the landslide volume is about 8700 m^3. The lithology is characterised by mudstone and sandstone. Dong-Yen Village is located close to the Yen-Feng bridge watershed (Fig. 3). The Yen-Feng bridge watershed is 17 km^2. The detail rainfall and flow discharge data of the Yeng-Feng Bridge watershed were also used to verify the hydrological parameters of SIMTOP model. The study area is 0.58 km^2 and average slope is 0.574. This area was subjected to multiple typhoons and rainstorms between 2010

Table 2 Rainstorm events for runoff simulation in the study area

Study watershed	Storm event	Peak rainfall depth (mm/h)	Cumulated rainfall depth (mm)	Duration (h)	Peak flow discharge (m^3/s)	Calibration/ verification
Shang-Gui-Shan Bridge	1996/07/30	43.94	603.99	51	2320	Calibration
	1997/08/28	37.64	481.94	42	1550	Verification
	1998/10/04	25.88	399.01	81	708	Verification
	2000/08/22	25.47	315.44	41	788	Verification
Yan-Feng Bridge	2012/08/07	64.50	128.00	26	131.75	Calibration
	2013/08/29	76.50	495.50	144	155.85	Verification
	2015/08/08	38.00	323.50	72	109.84	Verification
	2016/09/14	34.50	280.00	71	99.04	Verification

and 2016, including two severe shallow landslides caused by Typhoon Fanapi (2010) and Typhoon Megi (2016).

Model application

Model application

Table 2 shows the details of storm events that occurred in two study watersheds; these details were used for hydrological model's parameters calibration and model verification. The performance of the TOPMODEL was evaluated in terms of the runoff simulation results derived for the Shang-Gui-Shan Bridge (Fig. 2) and Yeng-Feng Bridge (Fig. 3) flow-gauging station. Four evaluation indices, namely error of peak discharge (EQ_p), error of time to peak discharge (ET_p), coefficient of efficiency (*CE*), and correlation coefficient (*CC*) were used to verify the applicability of the TOPMODEL for simulation rainfall–runoff and parameter calibration of SIMTOP. Simulation of an example rainstorm of the Shang-Gui-Shan Bridge watershed in 1996/07/30 is shown in Fig. 4. The simulated and observed hydrographs are in relatively good agreement in the both study watersheds. As shown in Table 3, the results showed that EQ_p is less than 15.9% in Yeng-Feng Bridge and 15.16% in Shang-Gui-Shan Bridge, ET_p is less than 1 h in the both study watersheds. *CE* is greater than 0.81, and *CC* is greater than 0.92. The analysis results revealed that the recession parameter m of the sample catchment area was 0.06 m; the hydraulic conductivity K_0 of the saturated soil was 5×10^{-3} m/s^2; and the maximum storage in the root zone S_{RZmax} was 0.02 m.

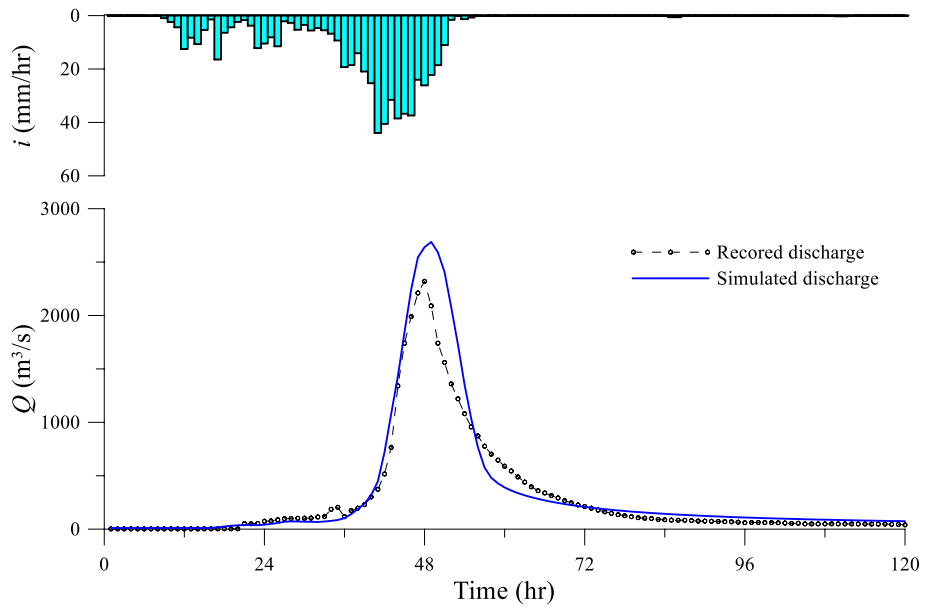

Fig. 4 Hydrograph simulation of the Shang-Gui-Shan Bridge watershed in 1996/07/30

Table 3 Runoff simulation results derived in the both study watersheds

Study watershed	Event date	EQ_p (%)	ET_p (%)	*CE*	*CC*
Shang-Gui-Shan Bridge	1996/07/30	15.9	1	0.88	0.98
	1997/08/28	6.1	−1	0.92	0.97
	1998/10/04	10.4	0	0.86	0.97
	2000/08/22	1.1	−1	0.81	0.97
Yan-Feng Bridge	2012/08/07	1.99	0	0.70	0.92
	2013/08/29	4.19	−1	0.91	0.96
	2015/08/08	14.41	−1	0.86	0.94
	2016/09/14	15.16	0	0.89	0.95

Because SIMTOP developed in this study combines the infinite slope stability model and the topographic hydrological model, detailed physiographic data of the catchment area were required for model calculations. Accordingly, this study adopted data from the 5 m × 5-m grid resolution to obtaining the required geomorphological factors by using the digital elevation model. This study verified the predictive ability of SIMTOP regarding shallow landslides. The parameters for the infinite slope stability analysis were determined through on-site sampling experiments and previous reports. They were set 30° for internal friction angle, 2.0 kPa for soil cohesive force, and 2000 kg/m^3 for soil bulk density. This set of model parameters was used for the simulation of the storm events during 2010–2017 in C1. Furthermore, the internal friction angle (30°), soil cohesive force (1.0 kPa), and soil bulk soil density (2000 kg/m^3) were used in the post hoc analysis in C2, and this parameter set was used in the 2009–2017 simulation.

Figure 5 illustrates the stability analysis of the C1. The blue histogram represents the hourly rainfall data, and red lines, respectively, indicate the variation of the mean *FS* ($\overline{FS}$). The data show the mean *FS* ($\overline{FS}$) changing with rainfall intensity; when the rainfall increases, more water infiltrated into soil and gradually raises the saturated water level to reduce the resistance force and the the mean *FS* ($\overline{FS}$), thus increasing the likelihood of shallow landslides. As shown in Fig. 5, between January 1, 2010 and October

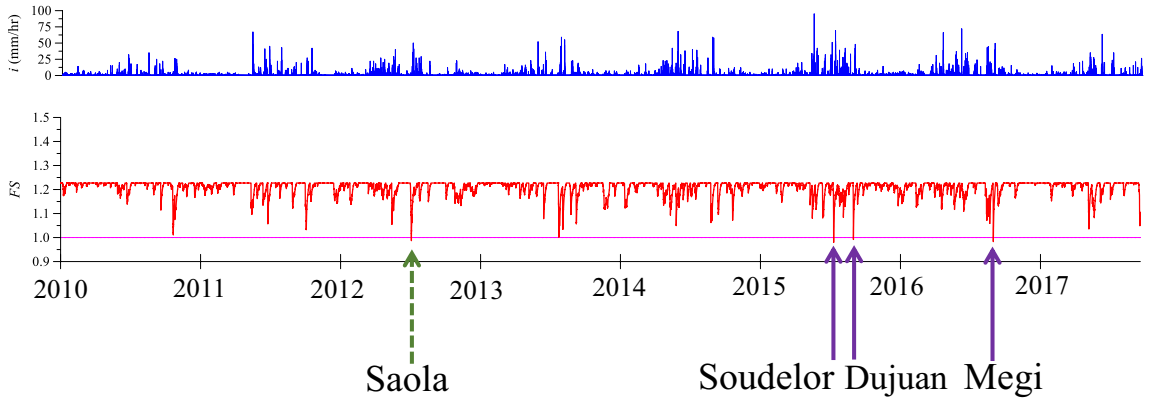

Fig. 5 Temporal variation of mean *FS* ($\overline{FS}$) in C1 from 2010 to 2017

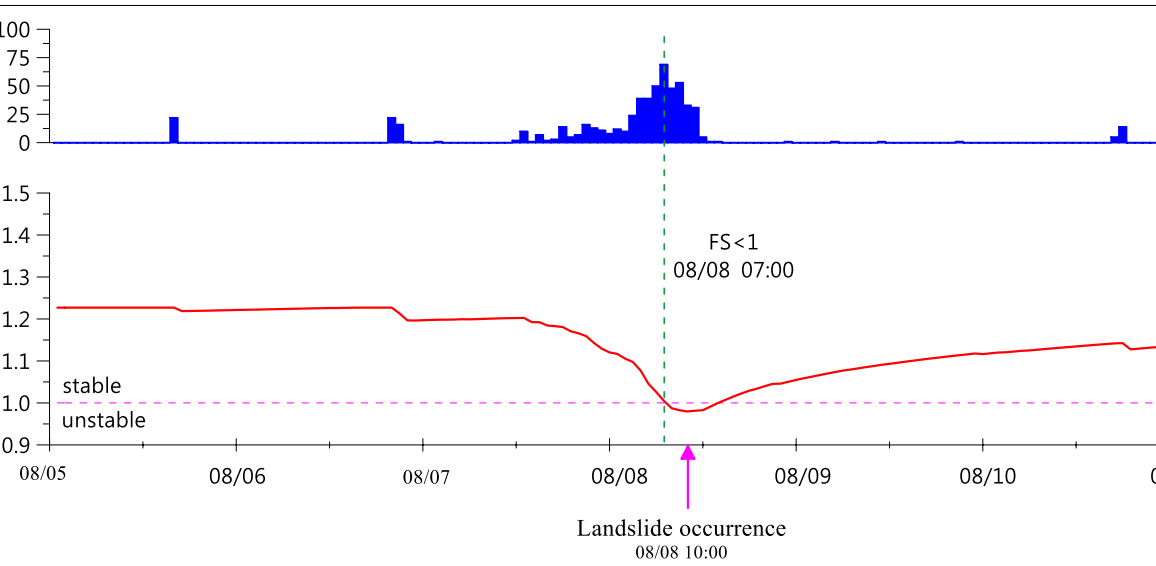

Fig. 6 Temporal variation of mean *FS* ($\overline{FS}$) in C1 during Typhoon Soudelor

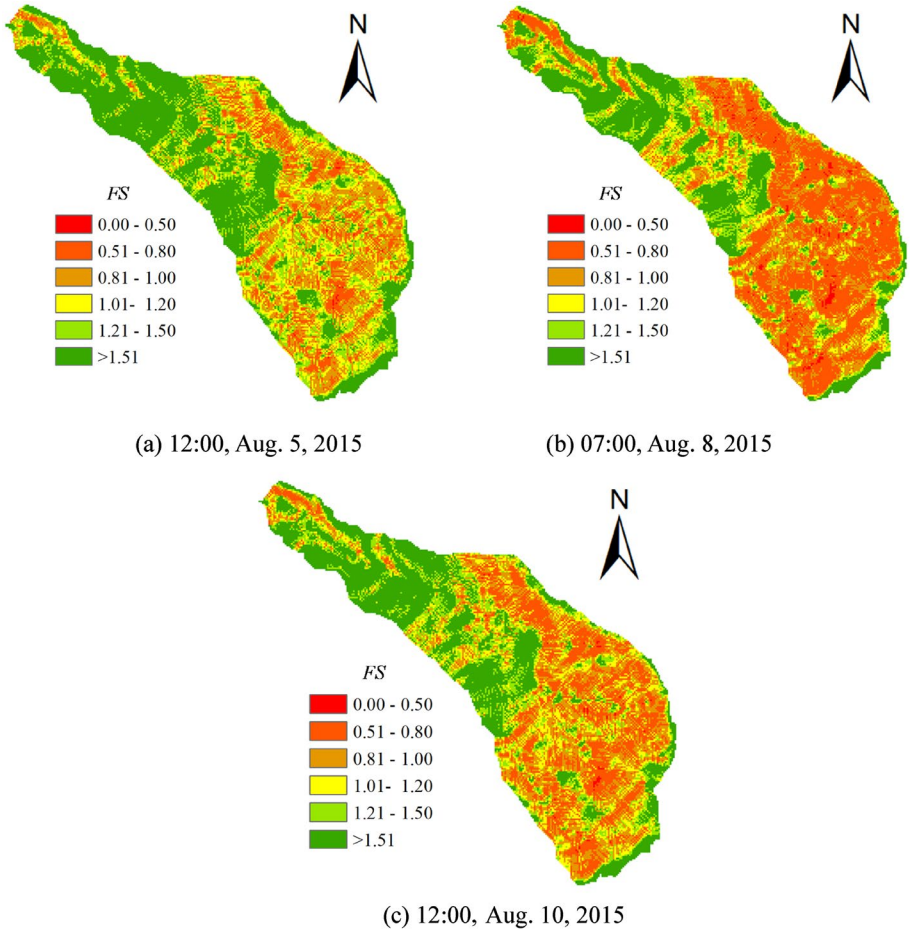

Fig. 7 Spatial distributions of the *FS* in C1 during Typhoon Soudelor

30, 2017, the mean *FS* ($\overline{FS}$) of C1 exceeded 1 at most of time, indicating stable states throughout the study period. However, the mean FS value was less 1 when Typhoon Saola (2012), Typhoon Soudelor (2015), Typhoon Dujuan (2015), and Typhoon Megi (2016) struck Taiwan. These findings reveal that C1 experienced unstable states during

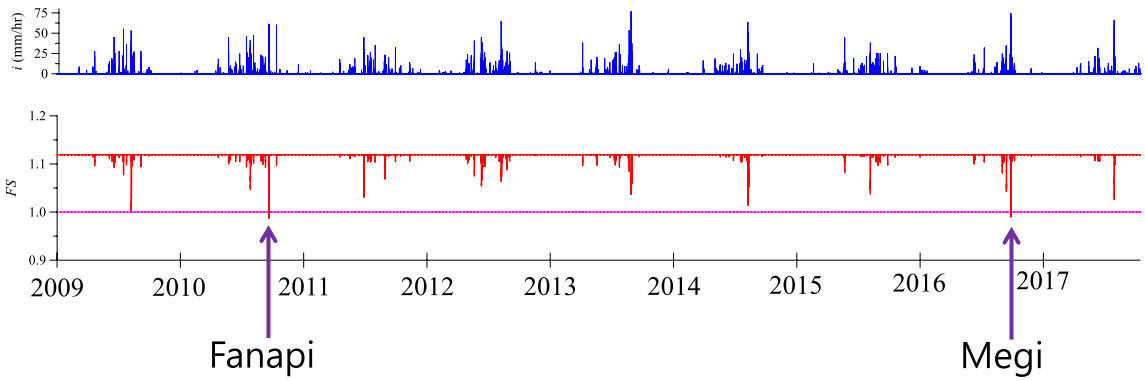

Fig. 8 Temporal variation of mean *FS* ($\overline{FS}$) in C2 from 2009 to 2017

the aforementioned typhoon events. The C1 matched the timing of documented shallow landslides occurrence. Figure 6 shows an example (Typhoon Soudelor, 2015) of the temporal variations of the mean *FS* ($\overline{FS}$) in C1. Figure 7 also presents the spatial distributions of the factor of safety (FS) generated from the SIMTOP model at C1 occurrence at (a) 12:00, Aug. 5 (initial); (b) 07:00, Aug. 8 (rainfall peak); and (c) 12:00 Aug. 10 (recession) during Typhoon Soudelor (2015). The results indicate the temporal variations of the mean *FS* ($\overline{FS}$) mainly follow the shape of the rainfall hyetograph because high rainfall intensity provides more water to infiltrate into soil to raise the groundwater table. Therefore, the shallow landslide timing predicted by the proposed model was determined to be consistent with the historical records.

During January 1, 2010 and October 30, 2017, C2 was also affected by two severe typhoons and resulted in landslides which were Typhoon Fanapi (2010) and Typhoon Megi (2015). As shown in Fig. 8, the SIMTOP model accurately predicted all the shallow landslide events generated by the Typhoon Fanapi (2010) and Typhoon Megi (2015) at C2.

TAPEX–SIMTOP integrated prediction and discussion

Fifteen typhoon events from 2014 to 2021 were selected for testing the applicability of the TAPEX–SIMTOP integrated prediction. This study applied the aforementioned data, as well as the timing of sea warnings corresponding to these 15 typhoons, to analyse and verify the performance of the ensemble rainfall forecasting model and the shallow landslide warning system. This study used the rainfall forecasts with a 6-h lead time at each time step (1 h). Moreover, this study used the real-time SIMTOP to calculate the mean FS of all ensemble units for the upcoming 1–6 h in C1 and C2. Consequently, this study adopted Eqs. 6 and 7 to determine the study area occur shallow landslide or not for the upcoming 6 h. As shown in Table 4, a comparison of the forecasts provided using the proposed model. For three typhoons

Table 4 Analysis results in C1 provided by the proposed model

Typhoon event	Warning period	Landslide occurrence	Times	Error matrix				Evaluation index		
				Hits	False alarms	Misses	No events	POD	FAR	TS
Chanthu	2021-09-10 05:30 2021-09-13 02:30	No	69	0	0	0	69	–	0.00	–
Hagupit	2020-08-10 10:30 2020-08-11 14:30	No	28	0	0	0	28	–	0.00	–
Lekima	2019-08-07 17:30 2019-08-10 08:30	No	63	0	0	0	63	–	0.00	–
Maria	2018-07-09 14:30 2018-07-11 14:30	No	48	0	0	0	48	–	0.00	–
Nesat	2017-07-28 08:30 2017-07-30 14:30	No	34	0	0	0	34	–	0.00	–
Megi	2016-09-25 23:30 2016-09-28 17:30	Yes	66	9	3	2	55	0.75	0.18	0.64
Malakas	2016-09-15 23:30 2016-09-18 08:30	No	57	0	0	0	37	–	0.00	–
Meranti	2016-09-12 23:30 2016-09-15 11:30	No	36	0	0	0	72	–	0.00	–
Nepartak	2016-07-06 14:30 2016-07-09 14:30	No	72	0	0	0	72	–	0.00	–
Dujuan	2015-09-27 08:30 2015-09-29 17:30	Yes	57	7	2	3	47	0.78	0.30	0.59
Soudelor	2015-08-06 11:30 2015-08-09 08:30	Yes	71	8	3	4	57	0.73	0.33	0.53
Chan-Hom	2015-07-09 05:30 2015-07-11 11:30	No	54	0	0	0	54	–	0.00	–
Linfa	2015-07-06 08:30 2015-07-09 05:30	No	69	0	0	0	69	–	0.00	–
Matmo	2014-07-21 17:30 2014-07-23 23:30	No	54	0	0	0	54	–	0.00	–
Fung-Wong	2014-09-19 08:30 2014-09-22 08:30	No	72	0	0	0	72	–	0.00	–

"–" denotes unavailability of POD and TS because the typhoon did not cause any landslides

Table 5 Analysis results in C2 provided by the proposed model

Typhoon event	Warning period	Landslide occurrence	Times	Error matrix				Evaluation index		
				Hits	False alarms	Misses	No events	POD	FAR	TS
Chanthu	2021-09-10 05:30 2021-09-13 02:30	No	69	0	0	0	69	–	0.00	–
Hagupit	2020-08-10 10:30 2020-08-11 14:30	No	28	0	0	0	28	–	0.00	–
Lekima	2019-08-07 17:30 2019-08-10 08:30	No	63	0	0	0	63	–	0.00	–
Maria	2018-07-09 14:30 2018-07-11 14:30	No	48	0	0	0	48	–	0.00	–
Nesat	2017-07-28 08:30 2017-07-30 14:30	No	34	0	0	0	34	–	0.00	–
Megi	2016-09-25 23:30 2016-09-28 17:30	Yes	66	6	1	2	57	0.85	0.14	0.67
Malakas	2016-09-15 23:30 2016-09-18 08:30	No	57	0	0	0	37	–	0.00	–
Meranti	2016-09-12 23:30 2016-09-15 11:30	No	36	0	0	0	72	–	0.00	–
Nepartak	2016-07-06 14:30 2016-07-09 14:30	No	72	0	0	0	72	–	0.00	–
Dujuan	2015-09-27 08:30 2015-09-29 17:30	No	57	0	0	0	57	–	0.00	–
Soudelor	2015-08-06 11:30 2015-08-09 08:30	No	71	0	0	0	71	–	0.00	–
Chan-Hom	2015-07-09 05:30 2015-07-11 11:30	No	54	0	0	0	54	–	0.00	–
Linfa	2015-07-06 08:30 2015-07-09 05:30	No	69	0	0	0	69	–	0.00	–
Matmo	2014-07-21 17:30 2014-07-23 23:30	No	54	0	0	0	54	–	0.00	–
Fung-Wong	2014-09-19 08:30 2014-09-22 08:30	No	72	0	0	0	72	–	0.00	–

"–" denotes unavailability of POD and TS because the typhoon did not cause any landslides

(Megi, Dujuan, and Soudelor) that induced landslides in C1, the following performance scores were obtained for the joint forecasts provided by the integrated model: minimum POD = 0.75; maximum FAR = 0.30; and minimum TS = 0.53. In addition, the joint forecasts precisely revealed that no landslide would occur during 12 other typhoons (i.e. no overestimation was observed). Therefore, the integrated model exhibited excellent performance in forecasting the time of shallow landslide occurrence in C1.

As shown in Table 5, only typhoon Megi induced the shallow landslide in C2 from 2014 to 2021, the following performance scores were obtained for the joint forecasts provided by the integrated model: POD = 0.85; FAR = 0.14; and TS = 0.67. In addition, the joint forecasts precisely revealed that no landslide would occur during 14 other typhoons. Therefore, the integrated model also exhibited excellent performance in forecasting the time of shallow landslide occurrence in C2.

Conclusion

The physically based SIMTOP developed in this study utilises high-resolution DEM data to construct a topographic hydrological model and a slope stability model. These two models simulate changes in saturated water levels in the soil and the FS of slopes in a catchment area during rainfall to predict the time and location of landslides in the catchment area. The proposed model considers not only the physiographic features of the catchment area, but also the effect of rainfall intensity on changes in saturated water levels to calculate the FS of the catchment area. The results of this study reveal excellent predictive performance in terms of the time of occurrence landslides in both study areas. Furthermore, to increase the disaster lead time, this study applied an ensemble rainfall forecasting model to predict precipitation in the catchment area with a 6-h lead time; this study integrated this model with SIMTOP to facilitate shallow

landslide forecasts, thereby yielding a comprehensive real-time landslide warning system for the catchment area. The following scores were obtained for simulations of 15 typhoon events in C1: POD $\geq$ 0.73; FAR $\leq$ 0.33; and TS $\geq$ 0.53; C2: POD = 0.85; FAR = 0.14; and TS = 0.67. Therefore, the proposed model may be applied to predict the occurrence time of potential disasters and extend the time available for disaster response, thereby mitigating loss of life and property.

Acknowledgements
The authors would like to thank the Taiwan Typhoon and Flood Research Institute and National Science and Technology Center for Disaster Reduction, Taiwan, for providing the rainfall forecasts and the Central Weather Bureau, Taiwan, for providing rainfall observation data.

Author contributions
J-YH, C-HL, W-BC, and C-HC validated the proposed model. KTL designed and performed the model. All authors contributed about equally to compose this paper, discussed the results, and commented on the manuscript at all stages. All authors read and approved the final manuscript.

Funding
This research was supported by the Soil and Water Conservation Bureau, Taiwan, under grant SWCB-105–159. The authors also acknowledge the financial support provided by the Ministry of Science and Technology in Taiwan.

Availability of data and materials
Vs data will be shared through the Soil and Water Conservation Bureau, Taiwan, after this paper is published.

Declarations

Ethics approval and consent to participate
The authors would like to confirm that they have no competing interest regarding this paper. All authors worked closely on this project starting from the conception of the project through modelling, analysis, interpretation of the results and write-up of the manuscript.

Consent for publication
Not applicable.

Competing interests
The authors declare that they have no competing interests.

Author details
[1]National Science and Technology Center for Disaster Reduction, New Taipei City, Taiwan. [2]Department of River and Harbor Engineering, National Taiwan Ocean University, Keelung, Taiwan. [3]Center of Excellence for Ocean Engineering, National Taiwan Ocean University, Keelung, Taiwan.

Received: 19 December 2021 Accepted: 18 May 2022
Published online: 03 June 2022

References

Apip TK, Yamashiki Y, Sassa K, Ibrahim HF (2010) A distributed hydrological-geotechnical model using satellite-derived rainfall estimates for shallow landslide prediction system at a catchment scale. Landslides 7:237–258
Beven KJ, Kirkby MJ (1979) A physically based variable contributing area model of basin hydrology. Hydrol Sci Bull 24(1):43–69
Caine N (1980) The rainfall intensity—duration control of shallow landslides and debris flows. Geogr Ann 62:23–27
Cannon SH, Ellen S (1985) Rainfall conditions for abundant debris avalanches San Francisco Bay Region. Calif Geol 38:267–272
Casadei M, Dietrich WE, Miller NL (2003) Testing a model for predicting the timing and location of shallow landslide initiation in soil-mantled landscapes. Earth Surface Process Landforms 28:925–950
Guzzetti F, Gariano SL, Peruccacci S, Brunetti MT, Marchesini I, Rossi M, Melillo M (2020) Geographical landslide early warning systems. Earth-Sci Rev 200:102973
Hsiao L, Yang M, Lee C, Kuo H, Shih D, Tsai C, Wang C, Chang L, Chen DY, Feng L, Hong J, Fong C, Chen D, Yeh T, Huang C, Guo W, Lin G (2013) Ensemble forecasting of typhoon rainfall and floods over a mountainous watershed in Taiwan. J Hydrol 506:55–68
Ho J-Y, Lee KT (2017) Performance evaluation of a physically-based model for shallow landslide prediction. Landslides 14(3):961–980
Hong Y, Adler R, Huffman G (2006) Evaluation of the potential of NASA multi-satellite precipitation analysis in global landslide hazard assessment. Geophys Res Letter 33:L22402
Iverson RM (2000) Landslide triggering by rain infiltration. Water Resour Res 36(7):1897–1910
Keefer DK, Wilson RC, Mark RK, Brabb EE, Brown W, Ellen SD, Harp EL, Wieczorek GF, Alger CS, Zatkin RS (1987) Real time landslide warning during heavy rainfall. Science 238:921–925
Kirkby MJ (1975) Hydrograph Modelling Strategies In: Process in Physical and Human Geography R Peel M Chisholm and P Haggett (Editors): 69–90
Lee KT, Ho J-Y (2009) Prediction of landslide occurrence based on slope instability analysis and hydrological model simulation. J Hydrol 375:489–497
Lee C-T, Huang CC, Lee JF, Pan KL, Lin ML, Dong JJ (2008) Statistical approach to storm event-induced landslide susceptibility. Nat Hazard Earth Syst Sci 8:941–960
Li J-S, Hong J-S (2011) The study of regional ensemble forecast: physical perturbations. Atmospheric Sci 39(2):95–115
Montgomery DR, Dietrich WE (1994) A physically based model for the topographic control on shallow landsliding. Water Resour Res 30(4):153–1171
Schaefer JT (1990) The critical success index as an indicator of warning skill. Weather Forecasting 5:570–575
Silalahi FES, Pamela AY, Hidayat F (2019) Landslide susceptibility assessment using frequency ratio model in Bogor, West Java Indonesia. Geoscience Lett 6:10
Skempton AW, Delory FA (1957) Stability of natural slopes in London clay. ASCE J 2:378–381
Wieczorek GF (1987) Effect of rainfall intensity and duration on the debris flows in central Santa Cruz Mountains California. Geo Soc Am Rev Eng Geol 7:93–104
Wilks DS (2005) Statistical methods in the atmospheric sciences, second ed., Elsevier.
Wu W, Sidle R (1995) A distributed slope stability model for steep forested basins. Water Resour Res 31(8):2097–2110
Zizioli D, Meisina C, Valentino R, Montrasio L (2013) Comparison between different approaches to modelling shallow landslide susceptibility: a case history in Oltrepo Pavese Northern Italy. Nat Hazard 13:59–573

Publisher's Note